Journal of Nuclear Materials 390–391 (2009) 211–215

Contents lists available at ScienceDirect

Journal of Nuclear Materials

journal homepage: www.elsevier.com/locate/jnucmat

Measurements of accumulated metallic impurities during LiTER operation in NSTX

S.F. Paul *, C.H. Skinner, J.A. Robinson, B. LeBlanc, H.W. Kugel

Princeton Plasma Physics Laboratory, Princeton University, Princeton, NJ 08543-0451, United States

ARTICLE INFO

PACS:
52.55.Hc
52.55.Fa
52.40.−w

ABSTRACT

Over 100 g of lithium was evaporated onto the NSTX plasma facing components using two stainless steel ovens (LiTER). Plasma emission was recorded using a 16-channel tangential bolometer and a VUV spectrometer. Confinement improved after lithium deposition and ELM's were either reduced or eliminated for hundreds of milliseconds. The radiated power profiles were generally, but not universally, highly peaked. Both peakness and a modeled on-axis high-Z impurity concentration were used as metrics for the degree of central metallic impurity accumulation. Several changes in plasma performance were seen, including reduction in plasma density and improvements in energy confinement, however high-Z impurity accumulation correlated most directly with ELM-suppression. In the more severe cases of accumulation, the volume-integrated radiated power exceeded 50% of the total input power and the estimated concentration of metals on-axis (modeled using iron as the representative impurity) reached 0.2% of the electron density.

1. Introduction

During the research campaigns over the last two years, one of the goals of the National Spherical Torus Experiment (NSTX) [1] program has been the investigation of the benefits that lithium coatings might have for both density and impurity control. Complementing the injection of lithium pellets [2], a more recent effort on NSTX has been using the LiThium EvaporatoR (LiTER) system to thermally evaporate lithium with the aim of coating a significant fraction of the plasma facing components. The benefits of depositing lithium, e.g. decreases in plasma density, inductive flux consumption, amplitude and frequency of edge-localized modes (ELM) [3] and MHD activity in general were observed [4]. However, in a number of ELM-free H-mode plasmas, the central radiated power density exceeded 50% of the input power and the radiated power profiles were strongly peaked [5]. To further investigate these effects in the 2008 campaign, a second LiTER was installed to apply lithium coatings over a larger fraction of the lower divertor surface, doubling the evaporation rate to 10–70 mg/min [6]. The procedure in this second experiment is to introduce lithium slowly into a series of reproducible discharges and observe any changes that could be ascribed to the evaporation of the lithium on the PFC's.

This paper describes the effect of lithium evaporation on high-Z impurity accumulation in these discharges as measured by a 16-channel AXUV tangential bolometer array with 5–8 cm spatial-resolution [7]. A concern about using AXUV photodiodes to measure radiated power is the known reduction in sensitivity to photons with energies <30 eV [8]. To compensate, power emitted within 3 cm of the separatrix is multiplied by 2.6, as discussed in Ref. [7]. This edge-correction has little effect on the profile or the total radiated power for profiles that are highly peaked and about a 15% effect on total radiated power for profiles that are hollow. Radiated power profiles are calculated from an Abel inversion of the chord-integrated measurements from the bolometer. The Abel inversion is carried out by fitting the chord-integrated emissivity profile with a smoothed cubic spline before performing the differentiation. The method employed does not require equidistant data spacing and features a local smoothing parameter [7]. The amount of smoothing for each chord is typically about 3% of the signal strength of the central chords for a strongly radiating discharge. The bolometer data were complemented with VUV spectra taken with a SPRED spectrometer that views along a radial chord in the mid-plane [8].

2. LiTER experiments on NSTX

The 2008 campaign began after a vacuum opening during which the graphite surfaces were cleaned. Following that, NSTX was operated over a period of approximately two months without lithium. Thus at the beginning of the LiTER experiments, the PFC's were considered to be essentially uncoated graphite. Prior to the evaporation, reference conditions were set up to produce high-recycling H-mode plasmas with reproducible ELM activity. The operating conditions generated a deuterium-fueled plasma in a lower single null configuration, with 6 MW of NBI heating, a toroidal field of 0.5 T, a plasma current of 800 kA, a triangularity of 0.5, and an

* Corresponding author.
E-mail address: spaul@pppl.gov (S.F. Paul).

0022-3115/$ - see front matter © 2009 Elsevier B.V. All rights reserved.
doi:10.1016/j.jnucmat.2009.01.170

elongation of 1.8. After the series of reference discharges were taken, lithium was evaporated over the course of a few discharges with constant gas fueling, NBI power and timing, plasma current and toroidal field, so that the effects of the lithium deposition might be isolated.

The lithium was deposited for ~10 min prior to each shot, resulting in the deposition 100–700 mg. Depositing 100 mg would correspond to a thickness of 62 nm if averaged over the area of the lower divertor or 4.7 nm if averaged over the entire interior of NSTX. The LiTER ovens were operated continuously during the course of the experiment at a selected rate that was controlled by the oven temperature. In addition, shutters were installed to mask the ovens during He glow conditioning and throughout the discharge, thus exposing the vacuum surfaces for a controlled duration. This regimen was adopted to prevent co-deposition of helium or deuterium with the lithium, thus minimizing the release of gases from the wall during the following discharge.

3. Results of the experiment

Plasma parameters are shown in Fig. 1 for a reference discharge (129020) that was reproduced about twelve times prior to lithium deposition. Lithium was then evaporated at a rate of 160 mg per discharge from both LiTERs over ~25 discharges gradually depositing a thin lithium coating onto the graphite surfaces of the PFC's. After the lithium evaporation was begun, a gradual decrease in Ohmic flux consumption, an increase in stored energy and lengthening of the discharge duration were observed over several shots. [6] After five shots, by which time about 2 g of lithium had been evaporated, the ELMs became more sporadic The NBI power was reduced from 4 to 2 MW to avoid a beta collapse, and yet the stored energy was approximately the same, indicating a near doubling of the energy confinement time. The gas puffing had to be increased by a factor of 1.8–2.0 to avoid low-density locked modes, indicating a increase in particle pumping by the PFC's. Eighteen shots into the lithium regimen (shot #129038), 5.7 g of lithium had been evaporated and the ELM's were completely suppressed. In fact, the D_α radiation emitted from the lower divertor on this shot, superimposed in Fig. 1(e) virtually disappeared after ~0.21 s. The line-integrated electron density decreased by 25%, as seen in Fig. 1(a) and the plasma stored energy increased by 15%, as seen in Fig. 1(d). A later discharge (shot #129041), by which point 8.3 g of lithium had been evaporated, is also shown in Fig. 1. The NBI power was raised to 3 MW at $t = 0.45$ s as shown

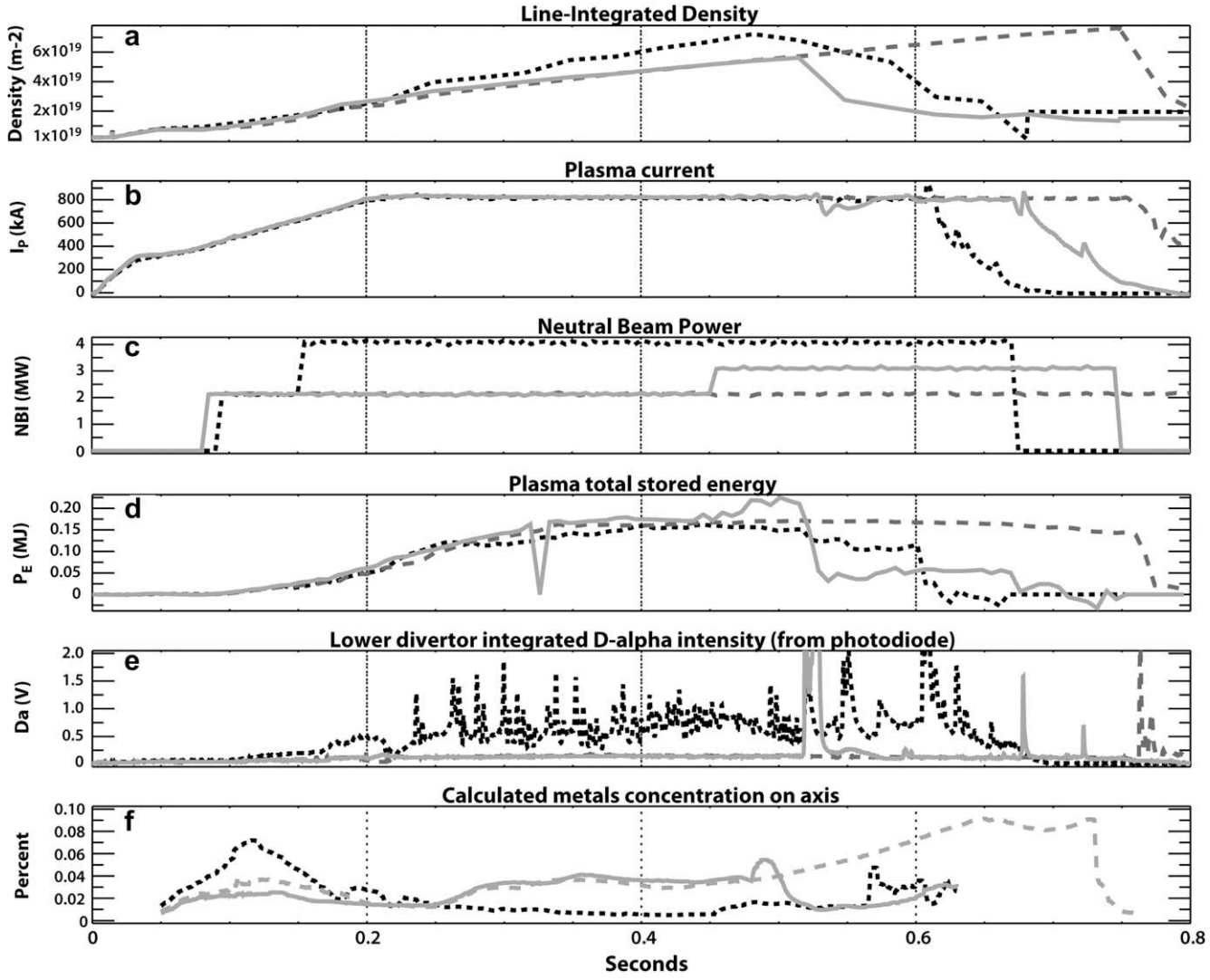

Fig. 1. Comparison of plasma parameters, (a) line-integrated density, (b) plasma current, (c) NBI power, (d) stored energy, (e) D_α emission and (f) calculated metals concentration on-axis for a reference shot (#129020) prior to lithium evaporation (dark dotted line) as well as #129038 (light solid line) and #129041 (light dashed line), which occurred 18 and 20 discharges after the initiation of lithium evaporation.

in Fig. 1(c). This discharge was also ELM-free and remained so even after the increase in NBI power, however the increase in stored energy caused the plasma to suffer a global beta collapse at ~0.52 s as seen in Fig. 1(d).

In Fig. 1(f), the calculated on-axis high-Z impurity concentration is shown for all three plasmas described above. This calculation employs a steady-state coronal-equilibrium model [9] to determine the concentration of impurities necessary to match the central radiated power density. The calculation assumes iron to be the sole radiating impurity in the center of the plasma, all low-Z radiators being fully stripped in the 1 keV core. Profiles of electron density, n_e, and temperature, needed for the calculation, are obtained from the NSTX Thomson scattering diagnostic, typically having an error of about ±4% [10]. The n_e profiles are generally quite flat in the core, so in interpolating over the width of the low spatial-resolution bolometer profile should not contribute very substantial errors in the calculation of the impurity concentration. The variation of the radiative cooling rate over the temperature range of interest (0.4–1 keV) for iron is only 20%, so variations in electron temperature should not contribute significantly either. Early in the shot (@ 0.15 s) when n_e is the same in both plasmas, the metals concentration in the core of the reference discharge is greater (0.07%) than in the post-evaporation discharge (0.03–0.04%), i.e., the high-Z impurity concentration is reduced when lithium is deposited onto the walls. The relative levels are reversed later in the shot after the H-mode transition. Prior to lithium deposition, the metals concentration is approximately 0.008% and remains largely constant throughout the shot, though the plasma density is ramping up. In contrast, starting .05 s after the H-mode transition at .21 s in the first ELM-free shot (#129038), the metals concentration ramps up to a value as high as 0.04%. At 0.5 s, the metals concentration in the core ramps up at an even higher rate. Despite the relatively strong gas puffing, the iron concentration reaches about 0.09% @ 0.7 s. With continued evaporation, subsequent shots become longer and the central metals concentration is routinely seen to increase to 0.12% or more by the end of the discharge.

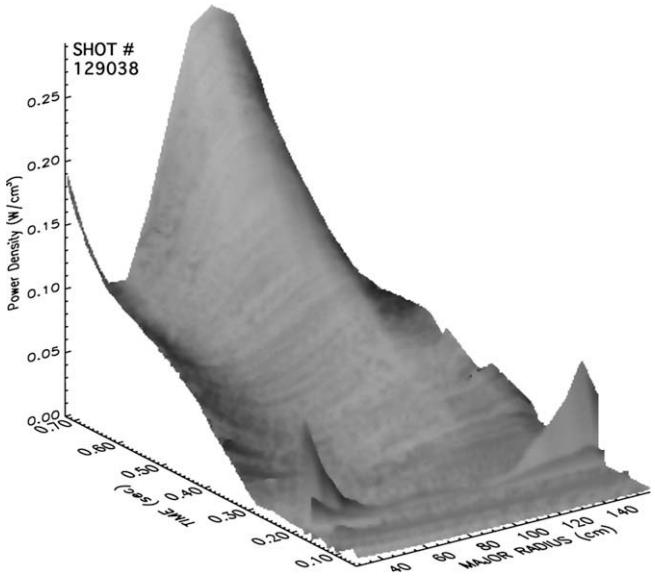

Fig. 2. Evolution of the radiated power density profile from first ELM-free shot, #129038.

Examining the radiated power profiles provides additional insight about the evolution of the impurities. During the ELMing period for the reference shot (#129020), the power density profile is hollow with the central power density remaining steady at about $2 \cdot 10^4$ W/m^3. The high-Z impurity confinement picture changes dramatically following 5.7 g of lithium evaporation. The 3D Abel-inverted profile of the radiated power density in the mid-plane is shown for ELM-free H-mode discharge #129038 in Fig. 2. Similar to the reference shot, the power density profile is hollow early in the shot (<0.48 s) and the central power density is only slightly higher ($2.5 \cdot 10^4$ W/m^3). At approximately 0.5 s, the radiated power density profile becomes strongly peaked (FWHM = approximately 50 cm @ 0.65 s) and the central power density increases to over $2.5 \cdot 10^5$ W/m^3. Though the power density profile is narrow (occupying a relatively small volume), the total radiated power reaches 1.4 MW, 70% of the total input power. The very high central power density leads to a reduction in the central electron temperature from 1000 to 750 eV (between a major radius of 0.6 and 1.3 m) as shown in Fig. 3.

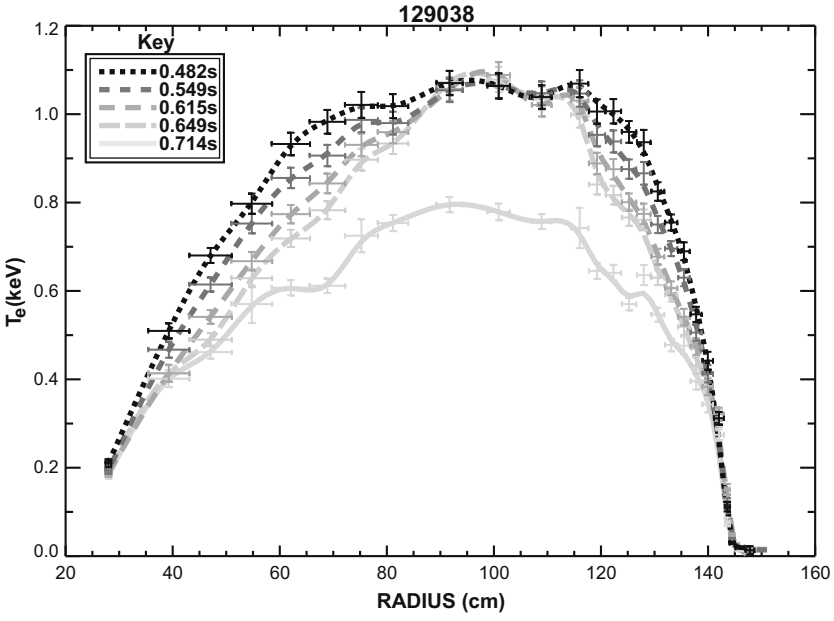

Fig. 3. Thomson scattering electron temperature profiles for shot #129038 from 0.5 to 0.7 s in 0.05 s intervals. The lightest curve is at the end of the shot.

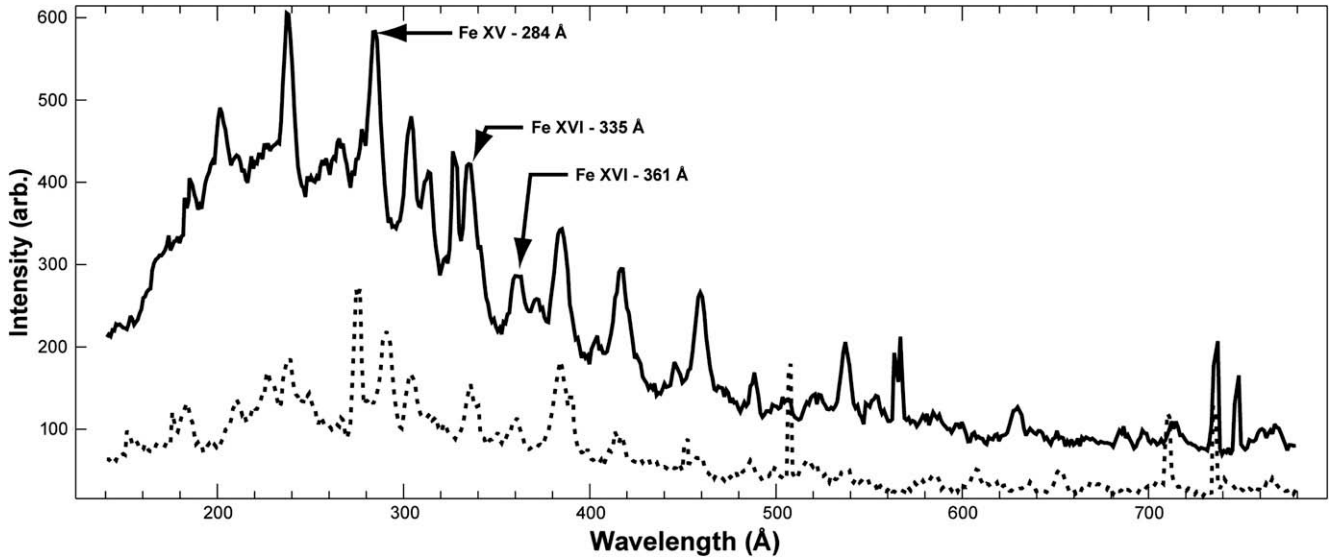

Fig. 4(a). VUV spectra at 0.45 s for the reference shot (#129020, dark, solid line) and for the first ELM-free shot following evaporation (#129038, light, dashed line).

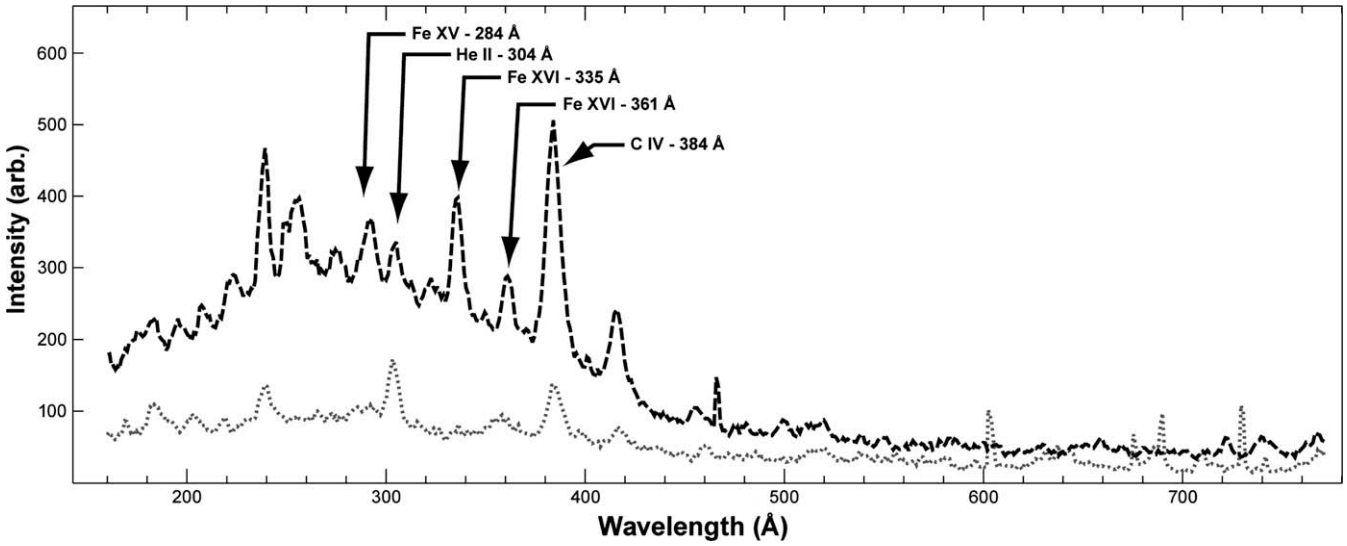

Fig. 4(b). VUV spectra at 0.73 s for the post-deposition (#129038 dark, solid line), and a similar post-deposition shot (#129041, light, dashed line) at 0.45 s.

In Fig. 4(a), the VUV spectra at 0.43 s from the reference shot and the first ELM-free shot after Li deposition are compared. The prominent lines in the reference shot are Fe XV and Fe XVI, representative of emission in an electron temperature range of 200–300 eV, i.e., the outermost 5 cm of the plasma. The SPRED spectrometer is not able to resolve the iron emission from the core of the plasma, e.g., Fe XXIII or Fe XXIV. The intensity of the broad feature in spectrum (a band of unresolved metallic lines) in the post-deposition is about four times less than the reference shot, substantially less than the 60% reduction that would expected just from the lower electron density. In addition, the iron lines are less prominent, suggesting that the lithium deposition reduces the generation of iron impurities. Fig. 4(b) compares the spectra of two post-deposition shots, one at 0.45 s and one at 0.74 s, showing that there is nearly a threefold increase in emission intensity, substantially *more* than the 40% increase that is expected from the higher density at the end of the shot. Note that this intensity is still only 75% of that in the reference shot in Fig. 4(a), despite having 20% higher electron density. Another difference is that most prominent line later in time is CIV @ 384 Å, implying that carbon becomes the dominant impurity at the edge.

4. Summary and conclusions

In ELMing H-mode shots prior to lithium deposition, metallic impurities are not observed to accumulate in the core of the plasma, despite a relatively high 0.08% concentration of metals in the core early in the shot and a large initial iron emission at the edge. The P_{rad} profiles remain very hollow throughout the shot and the core radiated power density is low, about $2 \cdot 10^4$ W/m^3.

Following Li evaporation, ELMs become sporadic and after 5–8 g of Li deposition, the ELM's disappear. The bolometer sees a lower concentration of metals initially, indicating some masking of the stainless steel surfaces by the deposited lithium. The reduced VUV emission indicates that the Li coating appears to have considerably reduced the influx of iron. Later in the shot, the electron density and the stored energy increase substantially and the radiated power density profile begins to fill in, eventually becoming sharply peaked. By the end of the shot, the core power density ex-

ceeds $2.50 \cdot 10^5$ W/m^3, indicating a strong accumulation of metals in a relatively small region near the core. By the end of the longer-duration ELM-free shots, the calculated concentration of iron-like metals routinely exceeds 0.1%, 5–10 times more than in the reference shots. The data from the VUV spectrometer show that the metals concentration and, even more so, the carbon concentration increase dramatically towards the end of the shot also. In this ELM-free high-confinement regime, more extensive graphite tile coverage will likely be required to moderate the influx of metals, so that the improved confinement seen with lithium deposition does not result in a radiative collapse of the plasma core.

Acknowledgments

The contributions from the entire NSTX research team are greatly appreciated. This work is supported by United States Department of Energy (US DOE) Contract DE-AC02-76CH03073.

References

[1] M.G. Bell, R.E. Bell, D.A. Gates, S.M. Kaye, et al., Nucl. Fusion 46 (2006) S565.
[2] H.W. Kugel, M.G. Bell, R. Bell, et al., J. Nucl. Mater. 363–365 (2007) 791.
[3] J.W. Connor, R.J. Hastie, H.R. Wilson, R.L. Miller, et al., Phys. Plasmas 5 (1998) 2687.
[4] H.W. Kugel, M.G. Bell, J.-W. Ahn, et al., Phys. Plasmas 15 (2008) 056118.
[5] S.F. Paul, Bull. Am. Phys. Soc. 52 (2007) 11 (paper TP8.00065).
[6] S.I. Krasheninnikov et al., Phys. Plasma 11 (2004) 3141.
[7] S.F. Paul, R. Maingi, V. Soukhanovskii, et al., J. Nucl. Mater. 337–339 (2005) 251.
[8] R.J. Fonck, A.T. Ramsey, R.V. Yelle, Appl. Opt. 12 (1982) 2115.
[9] D.E. Post, R.V. Jensen, C.B. Tarter, W.H. Grasberger, W.A. Lokke, Atom. Data Nucl. Data Tables 20397 (20) (1977) 397.
[10] B.P. LeBlanc, R.E. Bell, D.W. Johnson, et al., Rev. Sci. Instrum. 74 (2003) 1659.